On development of an efficient High-Level Green-Naghdi model for large-amplitude internal waves in deep waters

Z. Wang[1,2], T.Y. Zhang[1], B.B. Zhao[1,*], W.Y. Duan[1], M. Hayatdavoodi[1,3], R.C. Ertekin[1,4]

[1] College of Shipbuilding Engineering, Harbin Engineering University, Harbin, China
[2] Qingdao Innovation and Development Center of Harbin Engineering University, Qingdao, China
[3] School of Science and Engineering, University of Dundee, Dundee, UK
[4] Department of Ocean and Resources Engineering, University of Hawaii, Honolulu, USA

* zhaobinbin@hrbeu.edu.cn

Highlights

- A new High-Level Green-Naghdi (HLGN) model is derived to describe large-amplitude internal solitary waves for deep waters.
- Comparison between the present HLGN model and traditional HLGN model on wave profile and velocity field shows that the present HLGN model is more computationally efficient for large-amplitude internal solitary waves in deep waters.

1 Introduction

Internal solitary waves have been observed frequently in density stratified lakes and oceans. When the pycnocline depth is relatively small, the stratified ocean can be approximated as a two-layer fluid system. Meanwhile, the depth ratios of the upper- and lower-fluid depths h_2/h_1 (where h_1 and h_2 are the depths of the lower- and upper-fluid layers, respectively) in different ocean areas are quite different, which can even reach the ratio of 1:50, see e.g. Boyer et al. (2013).

For the study of large-amplitude internal solitary waves in shallow waters when $h_2/h_1 = O(1)$, the model derived by Miyata (1985) and Choi & Camassa (1996, 1999) (MCC model, hereafter) is widely used. Recently, Choi (2022) derived a second-order model to include the next-order correction to the MCC model. Good agreement was found between the results provided by the second-order model derived by Choi (2022) and Euler's solutions. Nevertheless, due to the long-wave assumption, the MCC model cannot be applied to solve internal solitary wave problem in deep waters when $h_2/h_1 << 1$.

For the study of large-amplitude internal solitary waves in deep waters, Choi & Camassa (1999) applied the linear theory to describe the lower-layer velocity field and developed an internal-wave model. Later, Debsarma et al. (2010) improved the dispersion property of this model. However, the results provided by the two models showed some differences with Euler's solutions (Debsarma et al., 2010). Zhao et al. (2016, 2020) developed the two-layer High-Level Green–Naghdi model for the large-amplitude internal solitary waves of finite depth (traditional HLGN model, hereafter). In this model, the variations of the horizontal and vertical velocities along the vertical direction are approximated by a series of polynomials. By comparing with the experimental data provided by Grue et al. (1999) and Michallet and Bathelemy (1998) and Euler's solutions, the traditional HLGN model was shown to describe accurately the large-amplitude internal solitary waves in both shallow and deep waters.

However, when applying the traditional HLGN model in deeper waters, e.g., from h_2/h_1 = 1/24 to 1/99, much higher-order polynomial terms are required to describe the velocity field of the lower-fluid layer accurately. In such cases, the number of unknowns increases and this affects the computational efficiency. Here, we are motivated to develop a new HLGN model where the exponential terms, instead of polynomials, are adopted to describe the vertical variation of velocity field of the lower-fluid layer.

This paper is organized as follows. The present HLGN model is described in Section 2. The comparisons between the present HLGN model and traditional HLGN model are presented and discussed in Section 3. Conclusions are reached in Section 4.

2 New internal wave model

A two-layer fluid system, which consists of two incompressible, immiscible and inviscid fluids, is considered. The origin of the Cartesian coordinate system is set at the undisturbed interface between the two-fluid layers. The mass densities of the upper and lower layers are ρ_2 and ρ_1, respectively. The upper-fluid layer is of finite depth and the lower-fluid layer is of infinite depth. The top surface of the upper-fluid layer and the interface between the two-fluid layers are written as $z = h$ and $z = \eta\ (x,\ t)$, respectively. The problem is set to be two dimensional. Sketch of this physical problem is shown in Fig. 1.

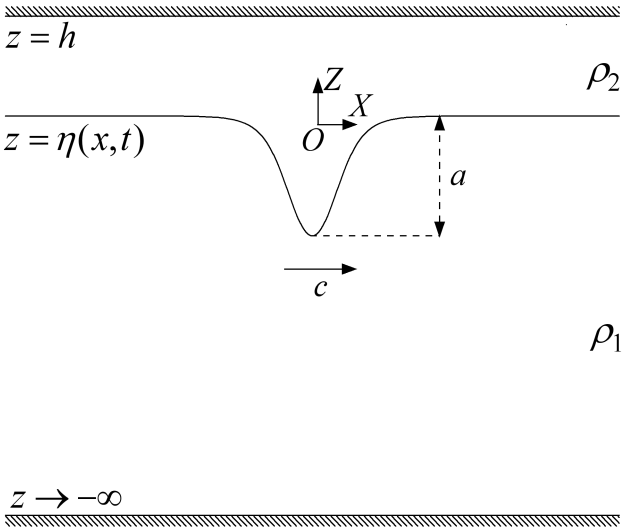

Figure 1 Sketch of a two-layer fluid system of infinite depth where the free surface is assumed to be a rigid lid

For each-fluid layer, the conservation equations of mass and momentum can be written as

$$\frac{\partial u}{\partial x}+\frac{\partial w}{\partial z}=0, \tag{1}$$

$$\frac{\partial u}{\partial t}+u\frac{\partial u}{\partial x}+w\frac{\partial u}{\partial z}=-\frac{1}{\rho}\frac{\partial p}{\partial x}, \tag{2a}$$

$$\frac{\partial w}{\partial t}+u\frac{\partial w}{\partial x}+w\frac{\partial w}{\partial z}=-\frac{1}{\rho}\frac{\partial p}{\partial z}-g, \tag{2b}$$

where u and w are the horizontal- and vertical-velocity components, respectively, p is the pressure and g is gravitational acceleration.

The kinematic boundary conditions are written as

$$w^{\mathrm{U}}=0, \quad z=h \tag{3a}$$

$$w^{\mathrm{U}}=\frac{\partial \eta}{\partial t}+u^{\mathrm{U}}\frac{\partial \eta}{\partial x}, \quad z=\eta(x,t) \tag{3b}$$

$$w^{\mathrm{L}}=\frac{\partial \eta}{\partial t}+u^{\mathrm{L}}\frac{\partial \eta}{\partial x}, \quad z=\eta(x,t) \tag{3c}$$

$$w^{\mathrm{L}}=0, \quad z\to-\infty \tag{3d}$$

where the superscripts U and L represent the variables related to the upper- and lower-fluid layer, respectively.

The dynamic boundary condition at the interface between the two-fluid layers is written as

$$\overline{p}^{\mathrm{U}}=\hat{p}^{\mathrm{L}}, \quad z=\eta(x,t) \tag{4}$$

where $\overline{p}^{\mathrm{U}}$ is the pressure at the lower surface of the upper-fluid layer and $\hat{p}^{\mathrm{L}}$ is the pressure at the upper surface of the lower-fluid layer.

In the traditional HLGN model, as shown in Zhao et al. (2016), the variations of the horizontal and vertical velocities along the vertical direction are approximated by a series of polynomials for each layer. In the present HLGN model developed in this paper, the variations of the horizontal and vertical velocities along the vertical direction are still approximated by a series of polynomials for the upper-fluid layer, while the variations of the horizontal and vertical velocities along the vertical direction of the lower-fluid layer are approximated by a series of exponential terms as

$$u^{\mathrm{U}}(x,z,t)=\sum_{n=0}^{K^{\mathrm{U}}-1}u_n^{\mathrm{U}}(x,t)z^n, \quad w^{\mathrm{U}}(x,z,t)=\sum_{n=0}^{K^{\mathrm{U}}}w_n^{\mathrm{U}}(x,t)z^n, \tag{5a}$$

$$u^{\mathrm{L}}(x,z,t)=\sum_{n=0}^{K^{\mathrm{L}}-1}u_n^{\mathrm{L}}(x,t)\mathrm{e}^{k_0 z}z^n, \quad w^{\mathrm{L}}(x,z,t)=\sum_{n=0}^{K^{\mathrm{L}}-1}w_n^{\mathrm{L}}(x,t)\mathrm{e}^{k_0 z}z^n, \tag{5b}$$

where K^{U} and K^{L} are the levels of the HLGN model that are applied to the upper- and lower-fluid layers, respectively. $k_0=2\pi/\lambda$ is the characteristic wavenumber and λ is the wavelength. In this paper, λ is selected by use of the MCC model.

The present HLGN model can be obtained by substituting Eq. (5) into Eqs. (1)-(4). The numerical algorithm for the travelling solutions is similar to that presented in Zhao et al. (2016).

3 Numerical results

In this section, we study a large-amplitude internal solitary wave in deep waters by using the present HLGN model and the traditional HLGN model. The parameters are as follows. Mass densities of the upper- and lower-fluid layers are $\rho_2 = 780\text{kg/m}^3$ and $\rho_1 = 1000\text{kg/m}^3$. Undisturbed depth of the upper-fluid layer and lower-fluid layer is 1m and 99m, respectively. The amplitude of the depression internal solitary wave is $a = -1.7955\text{m}$.

3.1 Convergence analysis of the present HLGN model

In this subsection, we test the convergence of the present HLGN model. The wave profiles and the horizontal velocity along the fluid column at the maximal displacement obtained by the present HLGN model with different levels are shown in Fig. 2.

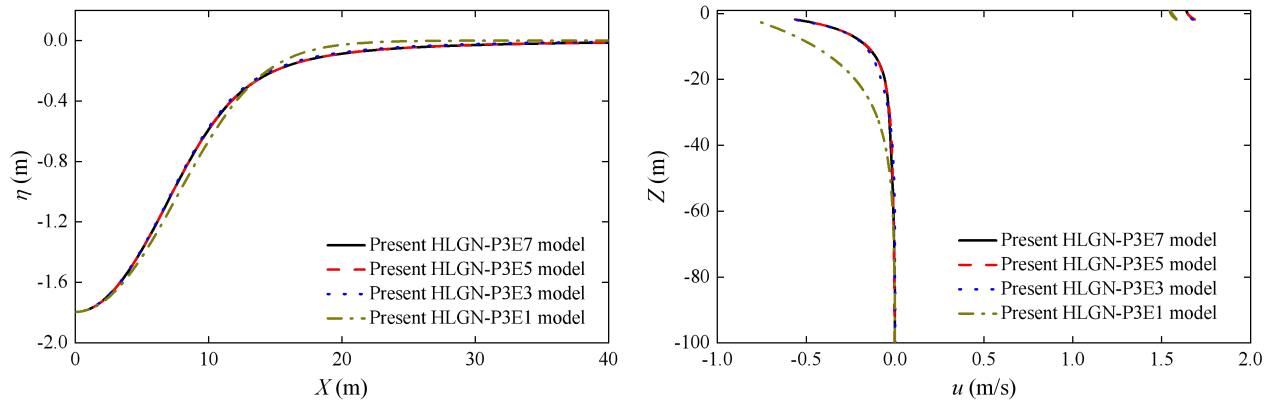

(a) Wave profile **(b) Horizontal velocity along the fluid column at the maximal displacement**

Figure 2 The convergence analysis of the present HLGN model

From Fig. 2, we observe that the results of the present HLGN-P3E5 model ($K^{\text{U}} = 3$ and $K^{\text{L}} = 5$ in Eq. (5)) agree well with the results of the present HLGN-P3E7 model. Thus, the results of present HLGN-P3E5 model are assumed to be the converged results of the present HLGN model.

Similarly, for the traditional HLGN model, we have also compared the results with different levels. We found that the results of the traditional HLGN-P3P8 model are the converged results of the traditional HLGN model. This indicates that the convergence is achieved at a lower level for the present HLGN model compared with the traditional HLGN model.

3.2 Comparisons between the present HLGN model and the traditional HLGN model

The comparisons between the results of the present HLGN model and the traditional HLGN model are shown in Fig. 3.

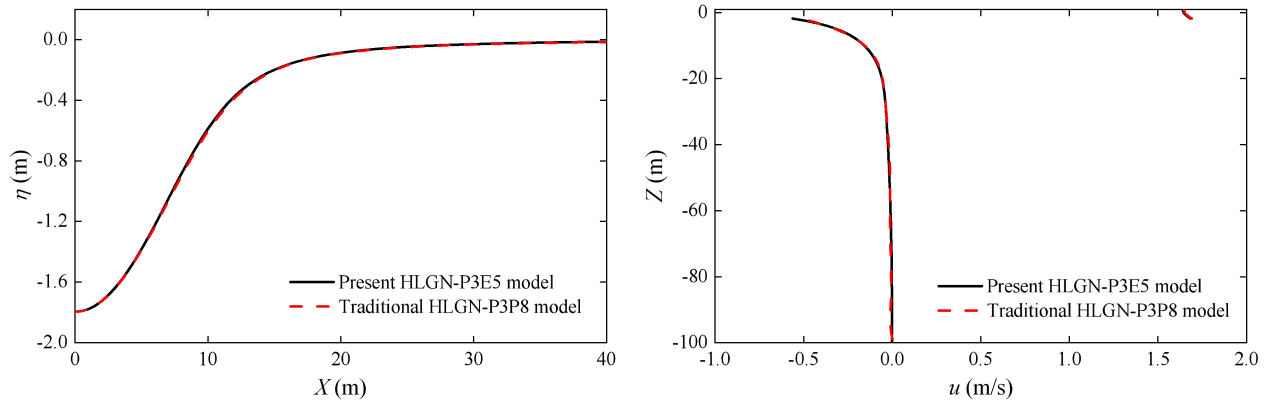

(a) Wave profile **(b) Horizontal velocity along the fluid column at the maximal displacement**

Figure 3 Comparison between the results of the present HLGN model and the traditional HLGN model

From Fig. 3, We observe that the results of the two models on the wave profile and velocity field show good agreement. However, it should be noted that the present HLGN model is more computationally effective because the number of unknowns is less than in the traditional HLGN model.

Next, we compared the CPU time of the present HLGN-P3E5 model and the traditional HLGN-P3P8 model in Table 1. In this paper, the number of calculated discrete points is 200 and the Newton-Raphson method is applied for solving the nonlinear equations. The numerical calculations are performed by use of *Mathematica* and the calculations were done on a laptop with an Intel (R) Xeon (r) W-11855M CPU@3.20GHz and 32GB of memory.

Table 1 CPU time of the present HLGN-P3E5 model and the traditional HLGN-P3P8 model

	Present HLGN-P3E5 model	Traditional HLGN-P3P8 model
CPU time	1.5 minutes	5 minutes

As shown in Table 1, under the same calculation conditions, the present HLGN model requires less CPU time, which verifies that the present HLGN model is more computationally efficient than the traditional HLGN model.

More information on the present HLGN model and the comparisons between the present HLGN model and other strongly nonlinear internal-wave models for the deep waters will be presented at the workshop.

4 Conclusions

In this paper, we develop a new HLGN model to describe the large-amplitude internal solitary waves in deep waters. The polynomials are applied to describe the variations of the horizontal and vertical velocities along the vertical direction of the upper-fluid layer of finite depth while the exponential terms are applied to describe the variations of the horizontal and vertical velocities along the vertical direction of the lower-fluid layer of infinite depth in this model. By comparing the results of the present HLGN model and the traditional HLGN model for the case of $h_2/h_1 = 1/99$, the calculated wave profiles and velocity fields show good agreement. The CPU time for the traditional HLGN-P3P8 model is about 5 minutes, while the CPU time for the present HLGN-P3E5 model is about 1.5 minutes. The present model is thus more efficient.

Acknowledgments

The first, third and fourth authors' (Z. Wang, B.B. Zhao and W.Y. Duan) work is supported by the National Natural Science Foundation of China (No. 12202114), the China Postdoctoral Science Foundation (No. 2022M710932), the State Key Laboratory of Coastal and Offshore Engineering, Dalian University of Technology (No. LP2202), the Heilongjiang Touyan Innovation Team Program and the Fundamental Research Funds for the Central Universities.

References

[1] Boyer, T.P., Antonov, O.K., Baranova, C., Coleman, C., Zweng, M.M. (2013). World Ocean Database 2013. NOAA Atlas NESDIS 72. 15.

[2] Miyata, M. (1985). An internal solitary wave with large amplitude. La Mar, 23: 43-48.

[3] Choi, W. & Camassa, R. (1996). Weakly nonlinear internal waves in a two-fluid system. Journal of Fluid Mechanics, 313: 83-103.

[4] Choi, W. & Camassa, R. (1999). Fully nonlinear internal waves in a two-fluid system. Journal of Fluid Mechanics, 396: 1-36.

[5] Choi, W. (2022). High-order strongly nonlinear long wave approximation and solitary wave solution. Part 2. Internal waves. Journal of Fluid Mechanics, 952, A41.

[6] Debsarma, S., Das, K.P., Kirby, J.T. (2010). Fully nonlinear higher-order model equations for long internal waves in a two-fluid system. Journal of Fluid Mechanics, 654: 281-303.

[7] Zhao, B.B., Ertekin, R.C., Duan, W.Y., Webster, W.C. (2016). New internal-wave model in a two-layer fluid. Journal of Waterway, Port, Coastal and Ocean Engineering, 142(3): 04015022.

[8] Zhao, B.B., Wang, Z., Duan, W.Y., Ertekin, R.C., Hayatdavoodi, M., Zhang, T.Y. (2020). Experimental and numerical studies on internal solitary waves with a free surface. Journal of Fluid Mechanics, 899, A17.

[9] Grue, J. (1999). Properties of large-amplitude internal waves. Journal of Fluid Mechanics, 380: 257-278.

[10] Michallet, H., and Barthelemy, E. (1998). Experimental study of interfacial solitary waves. Journal of Fluid Mechanics, 366(7): 159-177.